

The Light-activated Effect of Natural Anthraquinone Parietin against *Candida auris* and Other Fungal Priority Pathogens[#]



Authors

Johannes Fiala¹, Thomas Roach², Andreas Holzinger², Yurii Husiev³, Lisa Delueg¹, Fabian Hammerle¹, Eva Sanchez Armengol⁴, Harald Schöbel⁵, Sylvestre Bonnet³, Flavia Laffleur⁴, Ilse Kranner², Michaela Lackner⁶, Bianka Siewert¹

Affiliations

- 1 Department of Pharmacognosy, Institute of Pharmacy, Center for Molecular Biosciences Innsbruck, University of Innsbruck, Austria
- 2 Department of Botany, University of Innsbruck, Austria
- 3 Leiden Institute of Chemistry, Leiden University, Netherlands
- 4 Department of Technology, Institute of Pharmacy, Center for Molecular Biosciences Innsbruck, University of Innsbruck, Austria
- 5 Department of Biotechnology, MCI Innsbruck, Austria
- 6 Institute of Hygiene und Medical Microbiology, Medical University of Innsbruck, Austria

Keywords

Xanthoria parietina, Teloschistaceae, parietin, aPDT, photo-antimicrobial, EUCAST, *Candida auris*, Metschnikowiaceae

received

July 19, 2023

accepted after revision

January 5, 2024

Bibliography

Planta Med 2024; 90: 588–594

DOI 10.1055/a-2249-9110

ISSN 0032-0943

© 2024. The Author(s).

This is an open access article published by Thieme under the terms of the Creative Commons Attribution-NonDerivative-NonCommercial-License, permitting copying and reproduction so long as the original work is given appropriate credit. Contents may not be used for commercial purposes, or adapted, remixed, transformed or built upon. (<https://creativecommons.org/licenses/by-nc-nd/4.0/>)

Georg Thieme Verlag KG, Rüdigerstraße 14,
70469 Stuttgart, Germany

Correspondence

PD Dr. Bianka Siewert

Department of Pharmacognosy, Institute of Pharmacy, Center for Molecular Biosciences Innsbruck, University of Innsbruck
Innrain 80/82, 6020 Innsbruck, Austria

Phone: + 4 35 12 50 75 84 13, Fax: + 4 35 12 50 75 84 99

bianka.siewert@uibk.ac.at



Supplementary Material is available under
<https://doi.org/10.1055/a-2249-9110>

ABSTRACT

Antimicrobial photodynamic therapy (aPDT) is an evolving treatment strategy against human pathogenic microbes such as the *Candida* species, including the emerging pathogen *C. auris*. Using a modified EUCAST protocol, the light-enhanced antifungal activity of the natural compound parietin was explored. The photoactivity was evaluated against three separate strains of five yeasts, and its molecular mode of action was analysed via several techniques, i.e., cellular uptake, reactive electrophilic species (RES), and singlet oxygen yield. Under experimental conditions ($\lambda = 428$ nm, $H = 30$ J/cm², $PI = 30$ min), microbial growth was inhibited by more than 90% at parietin concentrations as low as $c = 0.156$ mg/L (0.55 μ M) for *C. tropicalis* and *Cryptococcus neoformans*, $c = 0.313$ mg/L (1.10 μ M) for *C. auris*, $c = 0.625$ mg/L (2.20 μ M) for *C. glabrata*, and $c = 1.250$ mg/L (4.40 μ M) for *C. albicans*. Mode-of-action analysis demonstrated fungicidal activity. Parietin targets the cell membrane and induces cell death via ROS-mediated lipid peroxidation after light irradiation. In summary, parietin exhibits light-enhanced fungicidal activity against all *Candida* species tested (including *C. auris*) and *Cryptococcus neoformans*, covering three of the four critical threats on the WHO's most recent fungal priority list.

Introduction

Members of the genus *Candida* are the most common causative agents of fungal infections [1, 2], representing a severe risk to human health [2, 3]. A relatively new human pathogenic species of this genus, i.e., *Candida auris*, was first isolated from a patient's

ear in Japan in 2009 [4]. Since then, reports of other *C. auris* infections rapidly occurred worldwide [5]. Infections are associated

[#] This work is dedicated to Professors Rudolf Bauer, Chlodwig Franz, Brigitte Kopp, and Hermann Stuppner for their invaluable contributions and commitment to Austrian Pharmacognosy.

ABBREVIATIONS

aPDT	antimicrobial photodynamic therapy
CDC	Centers for Disease Control and Prevention
cdr1p	Candida drug resistance protein 1
cdr1p	Candida drug resistance protein 2
CLSM	confocal laser scanning microscopy imaging
DLS	dynamic light scattering
DMSO	dimethyl sulfoxide
ECDC	European Centre for Disease Prevention and Control
EUCAST	European Committee on Antimicrobial Susceptibility Testing
HIV+	human immunodeficiency virus positive
MB	methylene blue
MDA	malondialdehyde
mdr1p	multidrug resistant 1 protein
MIC	minimal inhibitory concentration
NCAC	non-Candida albicans Candida species
NICD	national Institute for Communicable Diseases
PAHO	Pan American Health Organization
PS	photosensitizer
RB	rose bengal
RES	reactive electrophilic species
ROS	reactive oxygen species
TBO	toluidine blue O
WHO	World Health Organization

with crude mortality rates ranging from 28 to 66% [6], as physicians are confronted with a fungus that shows high rates of resistance against first-line and emergency therapy [7]. Furthermore, treatments are impeded by diagnostic challenges in species identification. Since 2016, governmental institutions (the Centers for Disease Control and Prevention (CDC), European Centre for Disease Prevention and Control (ECDC), World Health Organization (WHO), Pan American Health Organization (PAHO), and National Institute for Communicable Diseases (NICD)) have stressed the clinical relevance of *C. auris* infections to healthcare facilities and issued interim guidelines for clinical management, laboratory testing, and infection control [6,8,9]. However, the so-called “superbug” *C. auris* [10] is not the only common human pathogen with reported resistance development [11,12]. Also, non-*Candida albicans* *Candida* species (NCAC) such as *Candida glabrata* and *Candida tropicalis* [1,8], as well as the non-*Candida* yeast *Cryptococcus neoformans*, a pathogenic fungus spread through airborne spores, raise concerns [8,13]. Recently, *C. auris*, *C. albicans*, and *Cryptococcus neoformans* were listed in the critical priority group of the WHO’s fungal priority pathogens list to guide research, development, and public health action. *C. glabrata* and *C. tropicalis* were considered high-priority targets [8].

Increased use of antifungal drugs causes acquired resistance against these agents on top of the inherent primary resistance, thus making *Candida* species highly resistant to existing antifungal agents [11]. The number of antifungal agents is limited compared to available antibacterial agents, and most antifungal drugs are only fungistatic [12]. Although no improvement in survival rate

was found, fungicidal therapy of invasive *Candida* infections leads to a higher chance of therapeutic success and decreases the risk of recurrent infections, compared to fungistatic therapy alone [14].

Antimicrobial photodynamic therapy (aPDT) is an alternative approach to antifungal therapy with fungicidal properties. It is based on a different mechanism of action than established antifungal drugs [15]: the antifungal substance is inactive under dark conditions, but when exposed to visible light of corresponding wavelengths, it is activated and destroys pathogenic target cells. This approach, based on the synergistic effect of light and a chromophore, succeeds in killing multidrug-resistant microorganisms by causing multi-target damage through reactive oxygen species (ROS) [16]. According to the current state of knowledge, it can be assumed that aPDT is unlikely to promote relevant resistance in microorganisms [17–20], making this approach a promising treatment option in the fight against multidrug-resistant pathogens. With the help of a novel photoantimicrobial high-throughput screening (HTS) based on the European Committee on Antimicrobial Susceptibility Testing (EUCAST), our group recently reported the potential of fungal extracts containing the photosensitizer parietin to eradicate *Staphylococcus aureus* and *Candida albicans* [15]. Earlier reports showed parietin’s photoantimicrobial effect [21].

The aim of this study is to evaluate the potential of parietin as a photosensitizer (PS) against human pathogenic yeasts and to draw a comprehensive picture of its physicochemical and antimicrobial properties.

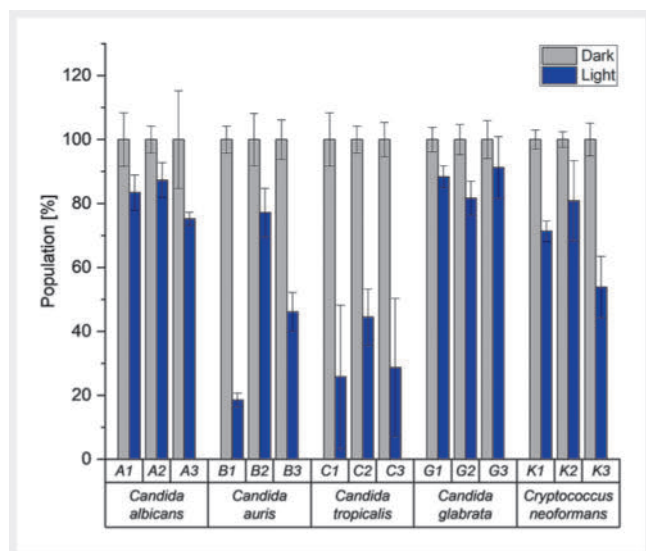
Results

Parietin (CAS 521–61–9) was isolated from freeze-dried samples of *Xanthoria parietina* by sonification in acetone and purified via a short sequence of chromatographic methods. The metabolite was obtained as yellow needles with a yield of 0.043% (see web-only Supplementary Figs. 1S and 2S).

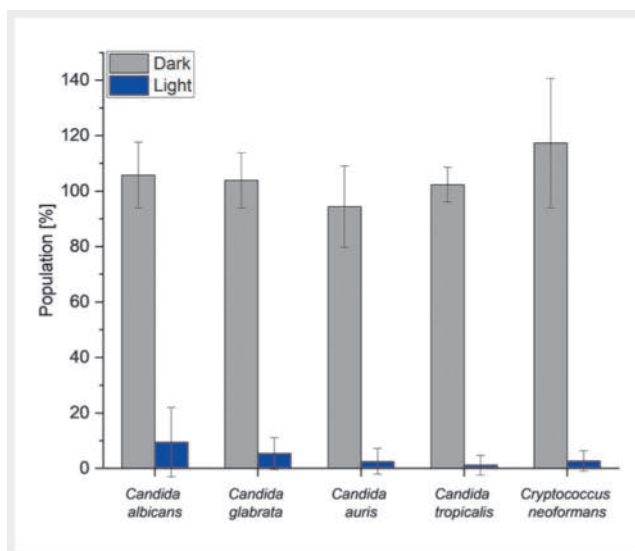
Frozen stock solutions of parietin in DMSO in lower concentrations undergo a decay over 29 days, while it is stable in higher concentrations: at a concentration of $c = 31.25$ mg/L (109.94 μ M), the highest decay (21.5%) was found. The lowest decay (7.39%) was determined for a concentration of $c = 125.00$ mg/L (439.74 μ M) (see web-only Supplementary Fig. 3S). Photostability experiments (see web-only Supplementary Fig. 4S) revealed a half-life of parietin (2.50 mg/L, 8.80 μ M, DMSO) under light irradiation ($\lambda = 430$ nm, 0.6785 mW) of $t_{1/2} = 133$ min ($H = 5.41$ J/cm²). A singlet oxygen photoyield (ϕ_{Δ}) of 94% was determined for parietin in deuterated methanol (see web-only Supplementary Fig. 5S).

Initial light toxicity experiments revealed a stronger effect of blue light alone on the viability of *C. auris* and *C. tropicalis* (60–80%), while the effect on other species was moderate (20–40%, ► Fig. 1). Intriguingly, *C. auris* showed a distinctive intra-strain susceptibility: strain B1 showed the highest sensitivity (82% reduced population); strain B2 instead was only moderately affected (23%) by blue light ($\lambda = 428$ nm, $H = 30$ J/cm²).

The average effect of parietin applied in the dark was negligible (<10% growth inhibition, $c_{\max} = 1.250$ mg/L, ► Fig. 2). However, when activated by light, parietin induced a strong inhibition of growth (>90%) in all five yeast species at a concentration of



► **Fig. 1** Graphical visualisation of the light toxicity, meaning the effect of light irradiation without PS on the growth of microorganisms ($\lambda = 428 \text{ nm}$, $H = 30 \text{ J/cm}^2$).



► **Fig. 2** Inhibition of growth achieved by parietin-based aPDT (1.250 mg/L, 4.397 μM) against five different species of yeast, averaged from three different strains per species. The grey bars represent the growth of the controls treated with parietin in the dark; blue bars denote parietin treatment in combination with light ($\lambda = 428 \text{ nm}$, $H = 30 \text{ J/cm}^2$, $PI = 30 \text{ min}$).

$c = 1.250 \text{ mg/L}$ (4.397 μM) (► **Table 1**, **Fig. 2**). For most strains, even smaller concentrations were sufficient (see web-only Supplementary **Fig. 6S**). For *C. glabrata*, a concentration of $c = 0.625 \text{ mg/L}$ (2.199 μM) led to an inhibition of growth of 91.1% (see web-only Supplementary **Fig. 7S**), and for *C. auris*, a parietin concentration of $c = 0.313 \text{ mg/L}$ (1.099 μM) killed 92.8% of the population (see web-only Supplementary **Fig. 6S**). Concentrations of $c = 0.157 \text{ mg/L}$ (0.550 μM) inhibited growth by 93.2% and 96.0% in *C. tropicalis* and *Cryptococcus neoformans*, respectively (see web-only Supplementary **Figs. 6S** and **7S**). Two of the *Candida albicans* strains (A1 and A2) showed the highest survival rates of all tested microorganisms (see web-only Supplementary **Figs. 8S** and **9S**). Interestingly, for strain A1, only a growth inhibition of 82.6% was obtained with concentrations up to $c = 1.250 \text{ mg/L}$ (4.397 μM) (see web-only Supplementary **Figs. 8S** and **9S**). Concentrations of $c = 2.500 \text{ mg/L}$ (8.795 μM) showed an adverse effect against all tested yeast populations besides strains of *Cryptococcus neoformans* and *C. tropicalis* (see web-only Supplementary **Figs. 9S–13S**).

Experiments with *C. albicans* (A1) showed that a longer pre-irradiation time of $t = 60 \text{ min}$ could not further increase the uptake of parietin (► **Fig. 3**). HPLC-DAD quantification of excess, wash, and uptake fractions allowed detailed tracking of parietin distribution.

CLSM imaging of *C. albicans* (A3) treated with 0.625 mg/L (2.199 μM) parietin (RPMI, 0.5% DMSO) confirmed that the cells associated with parietin (► **Fig. 4 a, b**). In addition, in a burst cell and remaining cell debris, parietin was located in the outer layers (► **Fig. 4 c, d**).

Quantification of reactive electrophilic species (RES) and aldehydes, both typical breakdown products of lipid peroxides, after irradiation experiments ($\lambda = 428 \text{ nm}$, $H = 30 \text{ J/cm}^2$, $PI = 30 \text{ min}$) against *Candida albicans* (A3) with the PS parietin (0.625 mg/L, 2.199 μM , in H_2O w/0.5% DMSO) showed a 10.6×10^2 -fold in-

► **Table 1** Overview of the antifungal effect of parietin under irradiation ($\lambda = 428 \text{ nm}$, $H = 30 \text{ J/cm}^2$) against the tested strains, *For *Candida albicans* (A1) with a concentration of 1.250 mg/L (4.40 μM), only an inhibition of growth of 83% was observed.

Work ID	Species	Parietin [mg/L] for aPDT inhibition of growth > 90%	Parietin [μM] for aPDT inhibition of growth > 90%
A1	<i>Candida albicans</i>	> 1.250*	> 4.397*
A2		0.625	2.199
A3		0.625	2.199
B1	<i>Candida auris</i>	0.157	0.550
B2		0.625	2.199
B3		0.313	1.099
C1	<i>Candida tropicalis</i>	0.313	1.099
C2		0.039	0.137
C3		0.039	0.137
G1	<i>Candida glabrata</i>	1.250	4.397
G2		0.625	2.199
G3		0.313	1.099
K1	<i>Cryptococcus neoformans</i>	0.078	0.275
K2		0.156	0.550
K3		0.078	0.275

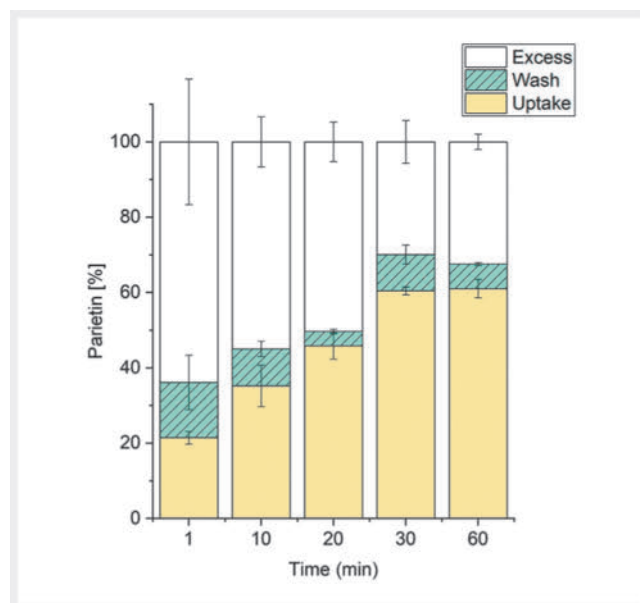
crease in 2-pentenal, compared to dark samples. Furthermore, increased values for acrolein (5.2×10^2 -fold), butyraldehyde (2.8×10^2 -fold), hexanal (2.7×10^2 -fold), malondialdehyde (MDA, 4.2×10^2 -fold), 2-hexenal (3.5×10^2 -fold), 2-nonenal (5.4×10^2 -fold), and 4-hydroxynonenal (5.7×10^2 -fold) were found (see web-only Supplementary Figs. 15S and 16S).

DLS experiments were performed in settings simulating the aPDT experiment (i.e., similar concentration range and medium). Up to the concentration of 1.25 mg/L (4.40 μ M), supramolecular aggregates of $2068.6 \text{ nm} \pm 14.0\%$ were found. Higher concentrations of parietin in RPMI with 0.5% DMSO led to larger particles (10.00 mg/L, $29060.0 \text{ nm} \pm 7.7\%$) (see web-only Supplementary Fig. 17S). Rodlike parietin formations could be observed by fluorescence microscopy starting at concentrations of 1.25 mg/L (4.40 μ M) (see web-only Supplementary Fig. 18S).

Discussion

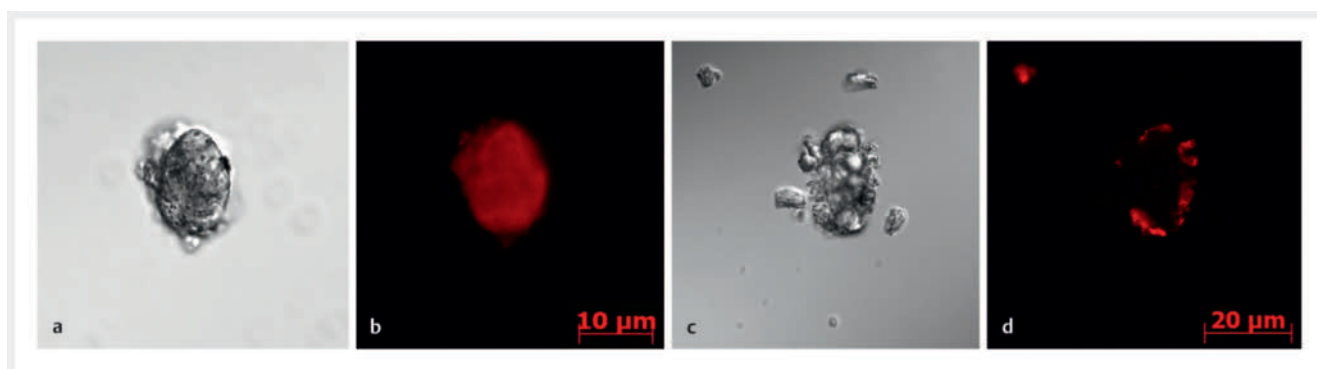
Candida species are opportunistic pathogens causing vaginitis, oral candidiasis, cutaneous candidiasis, candidemia, and systemic infections especially in immunosuppressed, diabetic, or HIV+ patients, but they can also affect healthy people [11]. Local infections, such as mucosal candidiasis, are generally easier to treat than systemic infections such as candidemia, which is one of the most common bloodstream infections in hospitals [22]. However, increasing numbers of drug-resistant *Candida* spp. infections are hampering the treatment of local infections, particularly in immunosuppressed patients. Photodynamic inhibition, or aPDT, is a topical treatment that has been shown to be successful and safe in clinical trials [23]. For example, in a recent study, the combined treatment of methylene blue, potassium iodine, and light was shown to improve the clinical course of oral *Candida* infections in AIDS patients [24]. In this clinical trial, up to 600 μ M of the drug methylene blue (MB, 191.91 mg/L) and a pre-irradiation time of five minutes were utilised [24].

The pre-irradiation time is thought to have no effect on the efficiency of aPDT treatments against bacteria [25]. For yeasts, however, the pre-irradiation time seems to be relevant and is considered to correlate with the intracellularisation of the photosensi-



► **Fig. 3** Uptake of parietin (1.25 μ g/mL/4.40 μ M) by *Candida albicans* (A1) after pre-irradiation times of 1/10/20/30/60 min. Parietin uptake is shown in yellow; parietin excess is shown in white. Turquoise sections represent the amount of parietin removable through washing in PBS.

tiser [15, 26]. Thus, the uptake of parietin was studied here in detail to determine the optimal pre-irradiation time ($t_{PI,opt}$) against *C. albicans*. Based on the observation that the internal content of parietin reaches its steady state after 30 minutes (► **Fig. 3**), an optimal pre-irradiation time ($t_{PI,opt}$) of 30 minutes was defined. The identified $t_{PI,opt}$ correlates to earlier reports [15, 27], where $t_{PI,opt}$ was determined based on the maximum log reduction reached. There are many putative reasons for this time dependency [27]. For example, the involvement of efflux pumps (Cdr1p and Cdr2p) has been proposed [11]. However, according to this rationale, a clear difference between susceptible and resistant strains at the defined t_{PI} should be observed. In this study, as in others [28], no



► **Fig. 4** Confocal laser scanning microscope (CLSM) imaging of *Candida albicans* (A3) treated with 0.625 mg/L (2.199 μ M) parietin (RPMI, 0.5% DMSO). (a) and (c) bright field images. (b) and (d) excitation was generated with an argon laser ($\lambda = 466 \text{ nm}$) and emission collected above $\lambda > 505 \text{ nm}$ and false-colourised red to visualise parietin distribution. (a) and (b) intact cell; (c) and (d) burst cell.

such difference was observed: the fluconazole-resistant *C. albicans* strain A1 (ATCC 64550) was as susceptible as the non-resistant strain A2 (ATCC 90028); see Fig. 8S (Supporting Information). Next to efflux pumps, the drug import may be mediated through transporters [29] or passive diffusion. However, the number of studies on drug uptake in fungal pathogens is limited. One described drug transporter is the *mdr1p* transporter, which is, however, also involved in fluconazole resistance [30].

Applying the identified $t_{PI,OPT}$ and the modified EUCAST protocol [15], promising PhotoMIC₉₀ values were defined for parietin: for the most robust species, *Candida albicans*, inhibition of growth occurred at $c = 1.250$ mg/L (4.397 μ M), whilst up to a concentration of $c = 400$ mg/L (1407.162 μ M) [31], no activity was reported under dark conditions. Photoantimicrobial inhibition (0.156 mg/L, 0.549 μ M) against *C. tropicalis* was over 600-fold smaller than reported under standard conditions (100 mg/L, 351.79 μ M, [31]), emphasising the synergistic effect of light and PS. For *Cryptococcus neoformans* (12.50 mg/L, 43.97 μ M, [31]), the photodynamic effect of parietin under irradiation (0.16 mg/L, 0.55 μ M) led to an 80-fold amplification of antimicrobial activity. For *C. auris* and *C. glabrata*, no published data about the antimicrobial activity of parietin could be found. In this study, we could show that under light irradiation >90%, growth inhibition was observed at $c = 0.313$ mg/L (1.10 μ M) against *Candida auris* and at $c = 0.625$ mg/L (2.20 μ M) against *Candida glabrata*, while in the dark and with the same concentrations, no activity > 10% was recorded. The EUCAST protocol [32] defines 0.5% DMSO as the final concentration for antimicrobial susceptibility testing, thus limiting the maximum concentration and therewith the possibility to determine an MIC under dark condition in this study due to solubility issues.

Parietin is a potent singlet oxygen producer ($\phi_{\Delta} = 94\%$, d4-MeOH), thus acting as a PDT type II photosensitiser, while slowly degrading under light irradiation (Fig. 4S, Supporting Information). Due to the lipophilic nature of parietin, it likely localised to the plasma membrane, in which the release of 1O_2 could lead to lipid peroxidation. Confocal laser scanning microscopy imaging indicated a cellular accumulation of parietin at the border layers of the cell (► Fig. 4). Unharmed, normal-shaped *Candida albicans* cells in the dark control samples were found with a size of 6 μ m (see web-only Supplementary Fig. 14S). Another anthraquinone-like photosensitiser (i.e., aloe-emodin) was reported to cause photodynamic damage through ROS to the cell envelope of *C. albicans* [33], corroborating the hypothesis of impairment of the cell membrane function as a mode of photoantimicrobial action. To test the hypothesis, analysis of 1O_2 -induced photooxidation products, so-called reactive electrophilic species (RES) and aldehydes, after aPDT irradiation were performed in this study. Oleic acid (26.0 \pm 3.0%), linoleic acid (30.0 \pm 3.0%), and linolenic acid (8.0 \pm 3.0%) are among the most relevant unsaturated fatty acids in *C. albicans* and together make up 64% of total fatty acids in plasma membranes of yeast [34]. Their photooxidation products acrolein, 2-pentenal, hexanal, 2-hexenal, and 2-nonenal (see web-only Supplementary Figs. 15S and 16S) were indeed increased after PDT treatment. Furthermore, the common lipid oxidation markers [34–37] MDA (4.22 $\times 10^2$ -fold increase), 4-hydroxynonenal (5.66 $\times 10^2$ -fold increase), and butyraldehyde

(2.77 $\times 10^2$ -fold increase) were significantly enhanced, confirming the hypothesis of the lipid oxidation being the mode of action.

Other groups have reported on the putative anticancer activity of parietin; for example, apoptosis and autophagy were induced by parietin in cells of a cervical cancer cell line (i.e., HeLa) with an EC₅₀ between 80 and 160 μ M (22.73 and 45.45 mg/L, respectively) in the dark [38]. In contrast, a PhotoEC₅₀ of $c = 30$ μ M was found for treatment (1 h) with parietin under blue light irradiation ($\lambda = 405$ nm, 3.08 J/cm²) against IGROV-1, another human ovarian cancer cell line [39]. However, as these reports are based on monolayer cell cultures, they are of limited relevance in estimating potential adverse effects of, e.g., skin lesion treatments. For example, a related chemical entity (i.e., the anthraquinone aloe-emodin) has recently been shown to be a potent photoantifungal agent against *Trichophyton rubrum* in an *in vivo* guinea pig model [40]. Investigations of the treated skin revealed no harmful side effects [40], despite several reports of aloe emodin's *in vitro* phototoxicity (e.g., [41, 42]). Thus, a straightforward estimation without a skin model based on the available literature data is not possible.

The observed high photoactivity of parietin against the pathogenic species *Candida auris* is, nevertheless, of special interest. Recently, another group described the photoantimicrobial effects of the well-established photosensitisers toluidine blue O (TBO, 400 μ M/122.33 mg/L), methylene blue (MB, 400 μ M/127.94 mg/L), and rose bengal (RB, 400 μ M/389.48 mg/L) against *C. auris* biofilms, reporting smaller inhibition of growth while using higher concentrations of the photosensitiser and stronger irradiation power (240 J/cm²) [43]. However, in the present study, the inhibition against planktonic cells was determined. Nevertheless, a concentration of $c = 0.625$ mg/L (2.199 μ M) killed 98.5% of a *C. auris* population ($\lambda = 428$ nm, H = 30 J/cm², PI = 30 min) (see web-only Supplementary Fig. 6S), while 8 mg/L (25.01 μ M) of MB were needed against planktonic cells ($\lambda = 635$ nm, 12 J/cm², PI = 60 min) [44]. Therewith, parietin is a promising new candidate to explore as a photosensitiser against *C. auris*. Local infections of the ear, as caused by *C. auris* [45], can be, for example, selectively treated utilising state-of-the-art light fibres, activating parietin solely in the spatial area of the light beam [46].

In conclusion, the present research shows that parietin concentrations in the low micromolar range (0.55–4.40 μ M/0.16–1.25 mg/L) are effective in killing different strains of the tested *Candida* spp. and *Cryptococcus neoformans* when combined with blue light ($\lambda = 428$ nm, H = 30 J/cm²). Furthermore, we present an experimental setup for the evaluation of the ideal pre-irradiation time. For *Candida albicans* with parietin, an assumed optimal pre-irradiation time of $t_{PI} = 30$ min could be confirmed. RES quantification showed the fungicidal effect of aPDT through the apparent damage of cell membranes. The photosensitising properties and aggregation behaviour of parietin in conditions of EUCAST antifungal susceptibility testing were characterised. Our work supports the search for urgently needed novel antimicrobials in the global fight against spreading resistance and shall offer new options for photosensitiser selection and research for aPDT. A major drawback of parietin is its limited solubility; however, future studies will investigate liposomal formulations.

Materials and Methods

Parietin was isolated from thalli of *Xanthoria parietina* through acetone extraction, crystallisation, size exclusion chromatography, and preparative HPLC (see web-only Supplementary Table 1S – 4S). Stability tests in DMSO were performed over 29 days in 7-day intervals. Photostability was tested via kinetic full spectrum measurement with a photometer over 24 h. Near-infrared emission measurements determined the singlet oxygen ($^1\text{O}_2$) yield (ϕ_Δ). Dynamic light scattering of parietin samples were measured in concentrations up to $c = 10.00$ mg/L (35.18 μM , RPMI with 0.5% DMSO). Photoantimicrobial broth microdilution experiments were performed as previously described [15], based on the adjusted EUCAST protocol for antifungal susceptibility testing [32] using a set of five yeast species (i.e., *Candida albicans*, *C. auris*, *C. glabrata*, *C. tropicalis*, and *Cryptococcus neoformans*; sources and further details are listed in Table 5S, Supporting Information), with three separate strains for each species. Uptake experiments were undertaken by incubating *C. albicans* cells (McFarland standard No. 1.5) with parietin ($c = 1.25$ mg/L, 4.40 μM , RPMI, 0.5% DMSO) at five different incubation times (1 min, 10 min, 20 min, 30 min, and 60 min). The final quantification of parietin was done via HPLC-DAD measurements. For fluorescence and confocal laser scanning microscopy, *C. albicans* cultures treated with parietin concentrations from $c = 0.625$ mg/L (2.20 μM) up to $c = 10.00$ mg/L (35.18 μM) were prepared. For quantifying reactive electrophile species (RES) and aldehydes after photoantimicrobial treatment, *C. albicans* suspensions adjusted to McFarland standard No. 2 and treated with parietin $c = 1.25$ mg/L (4.40 μM , water, 0.5% DMSO) were utilised. After irradiation ($\lambda = 428 \pm 15$ nm, $H = 30$ J/cm², $t_{PI} = 30$ min), samples were analysed by HPLC-DAD/MS.

Supporting Information

A detailed description of materials, instruments, and analytical and isolation methods are available as Supporting Information. Also, procedures for experiments on stability, singlet oxygen yield, aggregation, uptake, and photoantimicrobial activity of parietin are described, followed by the experimental conditions of CLSM and quantification of RES and aldehydes. Information on the tested strains, characterisation of parietin, and detailed results of the performed experiments, including an interpretation on the influence of the solubility of parietin, are provided.

Contributors' Statement

J.F. isolated and characterised parietin, performed all antifungal tests, contributed significantly to all other experiments, analysed the data, and wrote the first draft; T.R. performed and analysed the RES measurements; A.H. performed and analysed the CLSM experiments; Y.H. performed and analysed the singlet oxygen yield measurements; FH contributed to the characterisation of parietin; L.D. contributed significantly to the isolation of parietin; E.S.A. contributed to DLS measurement; H.S. developed the irradiation device for the photostability measurements; S.B. supervised the singlet oxygen measurements; F.L. supervised the DLS experiments; I.K. authenticated *X. parietina*, designed, super-

vised; ML designed and supervised the antimicrobial experiments, discussed the photoantimicrobial activity experiments, and edited the manuscript; BS designed and supervised, discussed, analysed data, and wrote and edited the manuscript.

Funding Information

This research was funded in whole or in part by the Austrian Science Fund (FWF) 10.55776/P31915 to BS and 10.55776/P34181 to AH. For open access purposes, the corresponding author has applied a CC BY public copyright license to any author accepted manuscript version arising from this submission.

Acknowledgements

We thank P. Vrabl, C. Schinagl, U. Peintner, and H. Stuppner for fruitful discussions.

Conflict of Interest

The authors declare that they have no conflict of interest.

References

- [1] Lass-Flörl C. The changing face of epidemiology of invasive fungal disease in Europe. *Mycoses* 2009; 52: 197–205
- [2] Silva S, Negri M, Henriques M, Oliveira R, Williams DW, Azeredo J. *Candida glabrata*, *Candida parapsilosis* and *Candida tropicalis*: biology, epidemiology, pathogenicity and antifungal resistance. *FEMS Microbiol Rev* 2012; 36: 288–305
- [3] Du H, Bing J, Hu T, Ennis CL, Nobile CJ, Huang G. *Candida auris*: Epidemiology, biology, antifungal resistance, and virulence. *PLoS Pathog* 2020; 16: e1008921
- [4] Satoh K, Makimura K, Hasumi Y, Nishiyama Y, Uchida K, Yamaguchi H. Antimicrobial photodynamic therapy in the treatment of oral candidiasis in HIV-infected patients. *Photomed Laser Surg* 2012; 30: 429–432
- [5] Lane CR, Seemann T, Worth LJ, Easton M, Pitchers W, Wong J, Cameron D, Azzato F, Bartolo R, Mateevici C, Marshall C, Slavin MA, Howden BP, Williamson DA. Incursions of *Candida auris* into Australia, 2018. *Emerg Infect Dis* 2020; 26: 1326–1328
- [6] Sears D, Schwartz BS. *Candida auris*: An emerging multidrug-resistant pathogen. *Int J Infect Dis* 2017; 63: 95–98
- [7] Ciurea CN, Mare AD, Kosovski IB, Toma F, Vintilă C, Man A. *Candida auris* and other phylogenetically related species – a mini-review of the literature. *Germs* 2021; 11: 441–448
- [8] World Health Organization. WHO Fungal Priority Pathogens List to Guide Research, Development, and Public Health Action. Geneva: World Health Organization; 2022
- [9] Clancy CJ, Nguyen MH. Emergence of *Candida auris*: An international call to arms. *Clin Infect Dis* 2017; 64: 141–143
- [10] Billamboz M, Fatima Z, Hameed S, Jawhara S. Promising drug candidates and new strategies for fighting against the emerging superbug *Candida auris*. *Microorganisms* 2021; 9: 634
- [11] de Oliveira Santos GC, Vasconcelos CC, Lopes AJO, de Sousa Cartágenes MDS, Filho A, do Nascimento FRF, Ramos RM, Pires E, de Andrade MS, Rocha FMG, de Andrade Monteiro C. *Candida* Infections and Therapeutic Strategies: Mechanisms of Action for Traditional and Alternative Agents. *Front Microbiol* 2018; 9: 1351
- [12] Oliveira JS, Pereira VS, Castelo-Branco D, Cordeiro RA, Sidrim JJC, Brilhante RSN, Rocha MFG. The yeast, the antifungal, and the wardrobe: A

- journey into antifungal resistance mechanisms of *Candida tropicalis*. *Can J Microbiol* 2020; 66: 377–388
- [13] Zafar H, Altamirano S, Ballou ER, Nielsen K. A titanic drug resistance threat in *Cryptococcus neoformans*. *Curr Opin Microbiol* 2019; 52: 158–164
- [14] Kumar A, Zarychanski R, Pisipati A, Kumar A, Kethireddy S, Bow EJ. Fungicidal versus fungistatic therapy of invasive *Candida* infection in non-neutropenic adults: A meta-analysis. *Mycology* 2018; 9: 116–128
- [15] Fiala J, Schöbel H, Vrabl P, Dietrich D, Hammerle F, Artmann DJ, Stärz R, Peintner U, Siewert B. A new high-throughput-screening-assay for photoantimicrobials based on EUCAST revealed unknown photoantimicrobials in cortinariaceae. *Front Microbiol* 2021; 12: 703544
- [16] Maisch T. Resistance in antimicrobial photodynamic inactivation of bacteria. *Photochem Photobiol Sci* 2015; 14: 1518–1526
- [17] Wozniak A, Rapacka-Zdonczyk A, Mutters NT, Grinholc M. Antimicrobials are a photodynamic inactivation adjuvant for the eradication of extensively drug-resistant *Acinetobacter baumannii*. *Front Microbiol* 2019; 10: 229
- [18] Al-Mutairi R, Tovmasyan A, Batinic-Haberle I, Benov L. Sublethal photodynamic treatment does not lead to development of resistance. *Front Microbiol* 2018; 9: 1699
- [19] Marasini S, Leanse LG, Dai T. Can microorganisms develop resistance against light based anti-infective agents? *Adv Drug Delivery Rev* 2021; 175: 113822. doi:10.1016/j.addr.2021.05.032
- [20] Rapacka-Zdonczyk A, Wozniak A, Pieranski M, Wozniowiczka A, Bielawski KP, Grinholc M. Development of *Staphylococcus aureus* tolerance to antimicrobial photodynamic inactivation and antimicrobial blue light upon sub-lethal treatment. *Sci Rep* 2019; 9: 9423
- [21] Comini LR, Morán Vieyra FE, Mignone RA, Páez PL, Laura Mugas M, Konigheim BS, Cabrera JL, Núñez Montoya SC, Borsarelli CD. Parietin: An efficient photo-screening pigment *in vivo* with good photosensitizing and photodynamic antibacterial effects *in vitro*. *Photochem Photobiol Sci* 2017; 16: 201–210
- [22] McCarty TP, White CM, Pappas PG. Candidemia and Invasive Candidiasis. *Infect Dis Clin North Am* 2021; 35: 389–413
- [23] Scwingel AR, Barcessat ARP, Núñez SC, Ribeiro MS. Antimicrobial photodynamic therapy in the treatment of oral candidiasis in HIV-infected patients. *Photomed Laser Surg* 2012; 30: 429–432
- [24] Du M, Xuan W, Zhen X, He L, Lan L, Yang S, Wu N, Qin J, Zhao R, Qin J, Lan J, Lu H, Liang C, Li Y, R Hamblin M, Huang L. Antimicrobial photodynamic therapy for oral *Candida* infection in adult AIDS patients: A pilot clinical trial. *Photodiagnosis Photodyn Ther* 2021; 34: 102310
- [25] Furtado GS, Paschoal MAB, Santos Grenho LC, Lago ADN. Does pre-irradiation time influence the efficacy of antimicrobial photodynamic therapy? *Photodiagnosis Photodyn Ther* 2020; 31: 101884
- [26] Andrade MC, Ribeiro APD, Dovigo LN, Brunetti IL, Giampaolo ET, Bagnato VS, Pavarina AC. Effect of different pre-irradiation times on curcumin-mediated photodynamic therapy against planktonic cultures and biofilms of *Candida spp.* *Arch Oral Biol* 2013; 58: 200–210
- [27] Jan A, Liu C, Deng H, Li J, Ma W, Zeng X, Ji Y. In vitro photodynamic inactivation effects of hypocrellin B on azole-sensitive and resistant *Candida albicans*. *Photodiagnosis Photodyn Ther* 2019; 27: 419–427
- [28] Paz-Cristobal MP, Royo D, Rezusta A, Andrés-Ciriano E, Alejandro MC, Meis JF, Revillo MJ, Aspiroz C, Nonell S, Gilaberte Y. Photodynamic fungicidal efficacy of hypericin and dimethyl methylene blue against azole-resistant *Candida albicans* strains. *Mycoses* 2014; 57: 35–42
- [29] Galocha M, Costa IV, Teixeira MC. Carrier-mediated drug uptake in fungal pathogens. *Genes (Basel)* 2020; 11: 1324
- [30] Sun N, Li D, Fonzi W, Li X, Zhang L, Calderone R. Multidrug-resistant transporter Mdr1 p-mediated uptake of a novel antifungal compound. *Antimicrob Agents Chemother* 2013; 57: 5931–5939
- [31] Tamokou JD, Tala MF, Wabo HK, Kuate JR, Tane P. Antimicrobial activities of methanol extract and compounds from stem bark of *Vismia rubescens*. *J Ethnopharmacol* 2009; 124: 571–575
- [32] Rodriguez-Tudela JL, Arendrup MC, Barchiesi F, Bille J, Chryssanthou E, Cuenca-Estrella M, Dannaoui E, Denning DW, Donnelly JP, Dromer F, Fegeler W, Lass-Flörl C, Moore C, Richardson M, Sandven P, Velegriaki A, Verweij P. EUCAST Definitive Document EDef 7.1: Method for the determination of broth dilution MICs of antifungal agents for fermentative yeasts. (Subcommittee on Antifungal Susceptibility Testing (AFST) of the ESCMID European Committee for Antimicrobial Susceptibility Testing (EUCAST)). *Clin Microbiol Infect* 2008; 14: 398–405
- [33] Ma W, Liu C, Li J, Hao M, Ji Y, Zeng X. The effects of aloe emodin-mediated antimicrobial photodynamic therapy on drug-sensitive and resistant *Candida albicans*. *Photochem Photobiol Sci* 2020; 19: 485–494
- [34] Marriott MS. Isolation and chemical characterization of plasma membranes from the yeast and mycelial forms of *Candida albicans*. *J Gen Microbiol* 1975; 86: 115–132
- [35] Biswas MS, Mano J. Lipid peroxide-derived reactive carbonyl species as mediators of oxidative stress and signaling. *Front Plant Sci* 2021; 12: 720867
- [36] Kato S, Shimizu N, Otaki Y, Ito J, Sakaino M, Sano T, Takeuchi S, Imagi J, Nakagawa K. Determination of acrolein generation pathways from linoleic acid and linolenic acid: Increment by photo irradiation. *NPJ Sci Food* 2022; 6: 21
- [37] Esterbauer H, Schaur RJ, Zollner H. Chemistry and biochemistry of 4-hydroxynonenal, malonaldehyde and related aldehydes. *Free Radic Biol Med* 1991; 11: 81–128
- [38] Trybus W, Król T, Trybus E, Stachurska A. Physcion induces potential anticancer effects in cervical cancer cells. *Cells* 2021; 10: 2029
- [39] Mugas ML, Calvo G, Marioni J, Céspedes M, Martínez F, Sáenz D, Di Venosa G, Cabrera JL, Montoya SN, Casas A. Photodynamic therapy of tumour cells mediated by the natural anthraquinone parietin and blue light. *J Photochem Photobiol B* 2021; 214: 112089
- [40] Ma W, Zhang M, Cui Z, Wang X, Niu X, Zhu Y, Yao Z, Ye F, Geng S, Liu C. Aloe-emodin-mediated antimicrobial photodynamic therapy against dermatophytosis caused by *Trichophyton rubrum*. *Microb Biotechnol* 2022; 15: 499–512
- [41] Lin HD, Li KT, Duan QQ, Chen Q, Tian S, Chu ESM, Bai DQ. The effect of aloe-emodin-induced photodynamic activity on the apoptosis of human gastric cancer cells: A pilot study. *Oncol Lett* 2017; 13: 3431–3436
- [42] Nowak-Perlak M, Ziolkowski P, Woźniak M. A promising natural anthraquinones mediated by photodynamic therapy for anti-cancer therapy. *Phytomedicine* 2023; 119: 155035
- [43] Bapat PS, Nobile CJ. Photodynamic therapy is effective against *Candida auris* biofilms. *Front Cell Infect Microbiol* 2021; 11: 713092
- [44] Tan J, Liu Z, Sun Y, Yang L, Gao L. Inhibitory effects of photodynamic inactivation on planktonic cells and biofilms of *Candida auris*. *Mycopathologia* 2019; 184: 525–531
- [45] Abastabar M, Haghani I, Ahangarkani F, Rezai MS, Taghizadeh Armaki M, Roodgari S, Kiakojuri K, Al-Hatmi AMS, Meis JF, Badali H. *Candida auris* otomycosis in Iran and review of recent literature. *Mycoses* 2019; 62: 101–105
- [46] Kim MM, Darafsheh A. Light sources and dosimetry techniques for photodynamic therapy. *Photochem Photobiol* 2020; 96: 280–294